Journal of the Serbian Chemical Society
JSCS@tmf.bg.ac.rs • www.shd.org.rs/JSCS
J. Serb. Chem. Soc. *90* (7–8) 957–972 (2025)
JSCS–5432
Original scientific paper
Published 29 July, 2025

Ruthenium(III)-monosubstituted Keggin-type polyoxotungstate: Synthesis, characterization and application in the catalytic methanation of carbon dioxide

SADIA MANSOURI[1,2] and SALEM CHEKNOUN[1,3]*

[1]*Laboratory of Applied Chemistry, Faculty of Science, M. Mammeri University, BP 17 RP, 15000 Tizi-Ouzou, Algeria,* [2]*Department of Chemistry, Faculty of Sciences and Applied Sciences, A.M. Oulhadj University, 10000 Bouira, Algeria and* [3]*Department of Chemistry Faculty of Science, M. Mammeri University, BP 17 RP, 15000 Tizi-Ouzou, Algeria*

(Received 18 February, revised 11 March, accepted 7 May 2025)

Abstract: $Cs_5[\alpha\text{-}SiW_{11}O_{39}Ru^{III}(H_2O)]\cdot 8H_2O$ heteropolysalt with a Keggin structure was successfully synthesized, and its physicochemical characteristics were determined *via* X-ray diffraction, UV–Vis spectroscopy, Fourier-transform infrared and Brunauer, Emmett and Teller surface area measurements. The acid––base properties were evaluated *via* isopropanol decomposition. The catalytic performance for the CO_2 methanation reaction was evaluated in a fixed-bed reactor at atmospheric pressure by varying the process parameters, which included the reaction temperature (200–450 °C), reactant mole ratio H_2/CO_2 (1, 2 and 4) and flow rate (1, 1.5 and 2 L/h). The experimental results showed that $Cs_5[\alpha\text{-}SiW_{11}O_{39}Ru^{III}(H_2O)]\cdot 8H_2O$ exhibited the best compromise between conversion and selectivity at 350 °C, with a H_2/CO_2 mole ratio of 4 and a flow rate of 1 L/h.

Keywords: Keggin-type polyoxometalate; hydrogenation; CO_2; methane.

INTRODUCTION

Polyoxometalates (POMs) are a large class of anionic metal oxygen clusters consisting of a transition metal called an “addenda atom” (*e.g.*, Mo, W and V in higher oxidation states), a heteroatom of a p-block element (usually Si or P) and a counteraction from group 1 (H^+, Li^+, Na^+, K^+ and Cs^+). POMs are known for their wide range of physicochemical properties, including strong acidity, redox behaviour, thermal stability and unique catalytic properties. These properties can be fine-tuned by the choice of heteroatoms, incorporated transition metals and counteractions, allowing the synthesis of a wide variety of structures.[1,2] These

* Corresponding author. E-mail: salem.cheknoun@ummto.dz
https://doi.org/10.2298/JSC250218034M

Available online at https://www.shd.org.rs/JSCS/

(CC) 2025 Serbian Chemical Society.

unique properties of POMs make them a class of materials with potential for catalytic applications.[3,4]

Owing to its excellent performance, Keggin, a well-known structure of POMs, has been tested as a catalyst for various reactions, such as oxidative dihydrogenation (ODH) of alkanes to alkenes[5,6] and arylalkanes to arylalkenes,[7] partial oxidation of methane to methanol,[8] oxidation of isobutane to methacrylic acid[9] and partial oxidation of propane to acrylic acid.[10]

Owing to the unique redox and catalytic properties of the ruthenium (Ru) atom, monoruthenium (Ru)-substituted Keggin-type heteropolytungstates have recently received considerable attention,[11] and they have been evaluated as catalysts for oxidation[12,13] and reduction reactions.[14]

Carbon dioxide is usually produced by combustion and is considered to be an important factor in the greenhouse effect and climate change. For this reason, carbon dioxide fixation has attracted much interest in recent years.[15,16] Although CO_2 has high thermodynamic stability, making it a particularly inert molecule, the hydrogenation reactions currently produce a number of useful chemical products, such as formic acid,[17] methanol[18] and methane,[19] depending on the different reaction conditions.

The Sabatier reaction (Eq. (1)), which converts carbon dioxide to methane, is the most thermodynamically favourable among carbon dioxide conversion reactions, with a negative change in Gibbs energy ($\Delta G_{298} = -130.8$ kJ/mol). However, owing to its high exothermicity ($\Delta H_{298} = -165$ kJ/mol), the complete reduction of carbon dioxide to methane needs low temperatures. Additionally, CO_2 reduction is an eight-electron process with notable kinetic constraints, requiring a suitable catalyst to achieve high reaction rates and methane selectivity:[20]

$$CO_{2(g)} + 4H_{2(g)} \rightarrow CH_{4(g)} + 2H_2O_{(g)} \quad (1)$$

Earlier studies have shown that transition metals such as Ru, Rh, Ni and Pd, particularly in groups VIII to X, are effective catalysts for producing methane through CO_2 hydrogenation, especially at lower temperatures.[20–22] Ni-based catalysts are commonly used because of their high activity, methane selectivity and low cost.[23,24] Ruthenium, while pricier, is more active than Ni and has high methane selectivity and low coke formation.[25]

In the present study, a Ru-POM catalyst was synthesized, characterized by various physicochemical techniques and tested for the CO_2 methanation reaction. The optimum conditions for CO_2 methanation were obtained by studying the effects of the reaction temperature, H_2/CO_2 molar ratio and gas mixture flow rate on the prepared catalyst.

(CC) 2025 Serbian Chemical Society.

EXPERIMENTAL

Materials

All chemicals and reagents used were of analytical grade and were acquired from Sigma Aldrich.

Preparation of $Cs_5[\alpha\text{-}SiW_{11}O_{39}Ru^{III}(H_2O)]\cdot 8H_2O$

The title compound was prepared *via* the use of Keggin-type monolacunary silicotungstate α-$K_8SiW_{11}O_{39}\cdot xH_2O$.

The monolacunary salt α-$K_8SiW_{11}O_{39}\cdot xH_2O$ (abbreviated SiW_{11}) was prepared *via* the following method.[26]

A 4 M solution of hydrochloric acid (165 mL) was added dropwise over 30 min, with vigorous stirring, to a solution of $Na_2WO_4\cdot 2H_2O$ (182 g) in 300 mL of boiling distilled water. To the resulting mixture, $Na_2SiO_3\cdot 5H_2O$ (11 g) in distilled water (100 mL) was added dropwise with stirring. The final solution was boiled for 1 h. After cooling to room temperature, KCl (150 g) was added to precipitate $K_8[SiW_{11}O_{39}]$. The white solid product was filtered, washed and finally dried in air. A polyhedral representation of a Keggin monolacunary anion, α-$SiW_{11}O_{39}^{8-}$ is shown in Fig. 1.

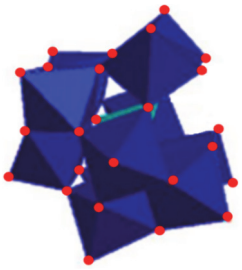

Fig. 1. Polyhedral representation of a Keggin monolacunary anion, α-$SiW_{11}O_{39}^{8-}$. Color code: WO_6 = dark blue octahedra, SiO_4 = teal tetrahedra and O = red.

The Keggin-type cesium salt of mono-ruthenium (III)-substituted silicotungstate, $Cs_5[SiW_{11}O_{39}Ru^{III}(H_2O)]\cdot 8H_2O$ (abbreviated as Cs-$SiW_{11}Ru$), was prepared *via* the literature method[27] with slight modifications. $RuCl_3$ (0.12 g) was dissolved in a minimal amount of water and added dropwise, with vigorous stirring, to a solution of 1.5 g of $[SiW_{11}O_{39}]^{8-}$ in 30 mL of water heated at 70 °C. The mixture was stirred for 60 min and then cooled to room temperature. Then, solid caesium chloride was added while stirring, and the black–brown precipitate was isolated, washed with methanol and dried under vacuum. A polyhedral representation of a Keggin anion $[\alpha\text{-}SiW_{11}O_{39}Ru^{III}(H_2O)]^{5-}$ is shown in Fig. 2.

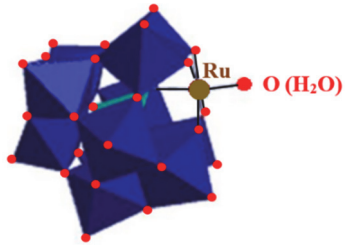

Fig. 2. Polyhedral representation of a Keggin anion $[SiW_{11}O_{39}Ru^{III}(H_2O)]^{5-}$; colour code: WO_6 = dark blue octahedra; SiO_4 = teal tetrahedron; Ru = brown and O = red.

(CC) 2025 Serbian Chemical Society.

Catalyst characterization techniques

The Brunauer, Emmett and Teller (BET) surface area (S_{BET}) was determined through N_2 adsorption–desorption analysis at a temperature of liquid N_2 (77 K) *via* a Quantachrome NOVA 4000e instrument. Approximately 10 mg of the catalyst sample was loaded into the U-shaped sample holder and degassed for 1 hour at 150 °C and 10^{-5} Pa in a N_2 gas flow to eliminate any adsorbed vapours. The surface area and pore size were determined by the BET theory and the Barrett–Joyner–Halenda (BJH) method, respectively.

The IR spectra of the samples were recorded on a Bio-Rad FTS 165 instrument *via* the KBr pellet technique in the region from 4000 to 400 cm^{-1}.

The fresh catalyst was analysed via X-ray diffraction (XRD) with a Siemens "D5000" diffractometer with a filtered CuKα X-ray source (λ = 1.5406 Å). The diffractogram was collected within a 2θ range of 0 to 60°.

The UV–Vis spectra of a 2×10^{-5} mol/L solution of the catalyst sample in neat acetonitrile were recorded with a Shimadzu UV-2100 PC spectrophotometer in the 190–400 nm range *via* quartz cuvettes with an optical path length of 10 mm.

The acid–base properties of the catalyst were determined through an indirect method, specifically the isopropanol (IPA) decomposition test. The test was conducted in a continuous--flow fixed-bed reactor at temperatures ranging from 100 to 200 °C under atmospheric pressure. Nitrogen (as the carrier gas) was passed through a saturator that contained IPA and maintained at 0 °C during the test. The catalyst weighed 200 mg, and the flow rate was 40 mL/min. The reaction products, which included propene, di-isopropyether and acetone, were analysed *via* a Shimadzu 14B gas chromatograph with a flame ionization detector (FID). The products were separated *via* 10 % Carbowax 20 M on Chromosorb W packed columns.

Catalytic tests

Catalytic experiments were conducted using 0.2 g of catalyst in a stainless-steel tubular fixed bed reactor measuring 6 mm in diameter and 400 mm in length for the gas-phase hydrogenation of carbon dioxide to methane. The reaction was carried out at atmospheric pressure by means of reaction mixtures of H_2/CO_2 with different molar ratios (1, 2 and 4) at temperatures ranging from 200 to 450 °C, and the flow rate of the reaction mixture ranged from 1 to 2 L/h. Prior to the activity tests, the catalyst was pre-treated in an oxygen stream at a flow rate of 2 L/h for 1 h at the reaction temperature. The reactants and products were analysed online by a Shimadzu GC-14 B gas chromatograph equipped with a TCD detector using a molecular sieve 5 Å packed column for the separation of H_2, CO_2, CO and CH_4. Data were collected after an 8-h reaction period. The experimental setup for the methanation of CO_2 is illustrated in Fig. S-1 of the Supplementary material to this paper. The performance of the catalyst was evaluated in terms of CO_2 conversion (X_{CO_2}) and CH_4/CO selectivity ($S_{CH_4/CO}$), which were determined *via* Eqs. (2) and (3), respectively:

$$X_{CO_2}\,(\%) = 100(\text{moles of } CO_{2in} - \text{moles of } CO_{2iout})/\text{moles of } CO_{2in} \quad (2)$$

$$S_{CH_4/CO}\,(\%) = 100(\text{moles of } CH_4/CO/\text{moles of all products}_{out}) \quad (3)$$

RESULTS AND DISCUSSION

Characterization of the catalyst

FT-IR Study. IR spectroscopy is a crucial and commonly utilized technique for characterizing POMs and confirming their structural integrity. Fig. 3 shows the

(CC) 2025 Serbian Chemical Society.

FT-IR spectra of SiW_{11} and Cs-$SiW_{11}Ru$. The IR spectrum of the mono-lacunary silicotungstate SiW_{11} exhibited five characteristic bands at 1000 cm^{-1} $\nu_{as}(W{=}O_t)$, 954 cm^{-1} $\nu_{as}(Si–O)$, 890 cm^{-1} $\nu_{as}(W–O_b–W)$ and 796 and 742 cm^{-1} $\nu_{as}(W–O_c–W)$, which agreed with those mentioned in the literature.[26]

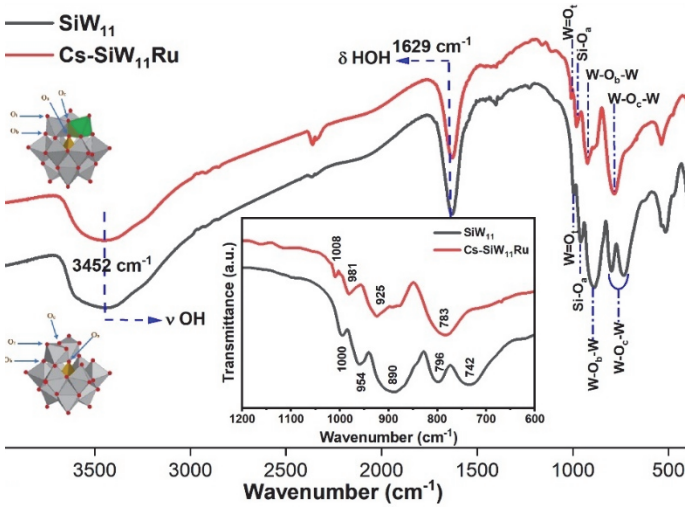

Fig. 3. FTIR spectra of $K_8(\alpha\text{-}SiW_{11}O_{39})$ (shown in black) and $Cs_5[SiW_{11}O_{39}Ru^{III}(H_2O)]$ (shown in red); insets: polyhedral representations of SiW_{11} and Cs-$SiW_{11}Ru$ with the corresponding metal–oxygen bonds were O_a: oxygen atoms attached to the silicon atom, O_t: terminal oxygen atoms bonded to the tungsten atom, O_b: oxygen atom belonging to the WO_6 octahedral units sharing corners and O_c oxygen atoms at the edges.

The IR spectrum of the monoruthenium-substituted Keggin silicotungstate Cs-$SiW_{11}Ru$ reveals that the POM anions are in the basic Keggin structure.[27,28] The four typical peaks at 1008, 980, 925 and 784 cm^{-1} are associated with $\nu_{as}(W{=}O_t)$, $\nu_{as}(Si–O_a)$, $\nu_{as}(W–O_b–W)$ and $\nu_{as}(W–O_c–W)$, respectively. The corresponding metal-to-oxygen bonding is displayed in the presented images. Furthermore, two prominent bands are observed at approximately 1630 and 3451 cm^{-1}, which can be attributed to the bending vibrations of water molecules (H–O–H) and the stretching vibrations of water hydroxyl groups (OH), respectively.

In the FT-IR spectrum of SiW_{11}, the stretching vibration of the W–Oc–W band was showed two distinct bands at 796 and 742 cm^{-1}. This splitting was caused by the decrease in structure symmetry (Cs symmetry) after the loss of one $[W{=}O]^{4+}$ group from the parent Keggin ion $(SiW_{12}O_{40})^{4–}$, characterized by Td symmetry.[29] In the FT-IR spectrum of Cs-$SiW_{11}Ru$, the main absorption bands were shifted toward higher wavenumbers and a only single band was observed for

(CC) 2025 Serbian Chemical Society.

the stretching vibration of W–Oc–W (*ca*. 783 cm^{-1}), which was due to the restoration of the classical α-Keggin type structure with Td symmetry,[30] indicating that the vacancy of the $SiW_{11}$was occupied by Ru(III).

UV–Vis spectra. Fig. 4 shows the UV spectra of SiW_{11} and Cs-$SiW_{11}Ru$, which display two absorption bands between 200 and 400 nm. The absorption peak at 227 nm is linked to charge transfer from terminal oxygen to metal atoms (Ot → W), whereas the absorption peak at 255 nm is associated with charge transfer from bridging oxygen to metal atoms (O_b/O_c → W). These distinct bands are characteristic of Keggin-type heteropolytungstates.[29,31] However, the absorption peak at 250 nm increased in intensity and became more distinct following the addition of the metal cation in the lacunary position, providing the evidence of the combination of α-SiW_{11} and Ru^{III}.

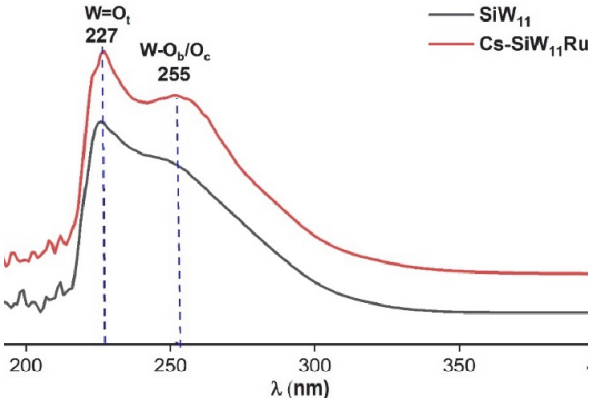

Fig. 4. UV–Vis spectra of $K_8(\alpha\text{-}SiW_{11}O_{39})$ and $Cs_5[SiW_{11}O_{39}Ru^{III}(H_2O)]$.

Powder XRD study. X-ray diffraction analysis is used extensively to study the structure of POMs. Fig. 5 shows the XRD patterns of solid $CsSiW_{11}Ru$. The sharp peaks demonstrate that Cs-$SiW_{11}Ru$ is crystalline. The diffractogram of Cs-$SiW_{11}Ru$ shows four groups of peaks at 2θ ranges of 7–10°, 16–22°, 25–30° and 33–38°, which are consistent with the characteristic diffraction peaks of the Keggin structure.[30,32] According to the literature,[28] the XRD pattern of Cs-$SiW_{11}Ru$ agrees with the existence of a single crystallographic phase with a pattern typical of a tetragonal system (space group *P*42/*ncm)* with a = 20.9299 Å, c = 10.3603 Å.

Textural properties of Cs-$SiW_{11}Ru$

N_2 adsorption–desorption isotherms and pore diameter distribution diagrams are depicted in Fig. 6, and the main results are shown in Table I. According to the IUPAC classification, the isotherm shape (Fig. 6A) of the synthesized salt was categorized as type IV, typical for mesoporous materials, with a hysteresis loop due

(CC) 2025 Serbian Chemical Society.

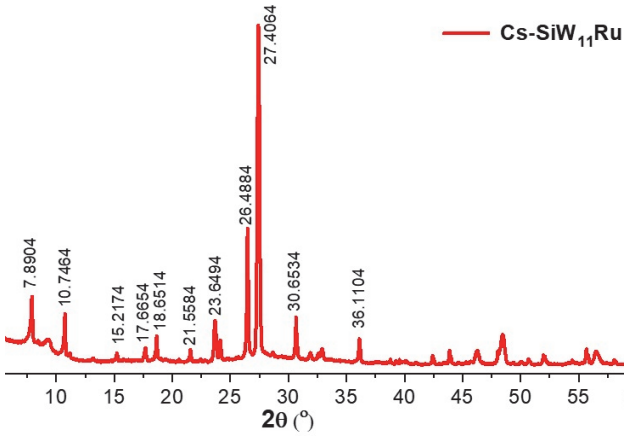

Fig. 5. X-ray diffraction pattern of the Cs-$SiW_{11}Ru$ catalyst.

TABLE I. Textural properties of the Cs-$SiW_{11}Ru$ catalyst

Solid	Specific surface $m^2\ g^{-1}$	Pore volume, V_{IP} $10^{-2}\ cm^3\ g^{-1}$	Pore diameter, d_m nm
Cs-$SiW_{11}Ru$	150.2	4.7	3.4

to the vaporization of nitrogen condensed in the mesopores.[31,33] Another interesting feature is the steep increase in adsorption at low pressures ($P/P_0 < 0.1$), which also suggests the presence of micropores in this sample.[32,34] From Fig. 6B, the pore size distribution curve shows a maximum at 3.4 nm, confirming that the salt was a mesoporous solid (*i.e.*, mesoporous solids between 2 and 50 nm). The textural parameters ($S_{BET} \approx 150\ m^2\ g^{-1}$, $V_p \approx 0.47\ cm^3\ g^{-1}$) of the sample are in agreement with reported values for Keggin-type silicotungstic cesium salt.[33,35]

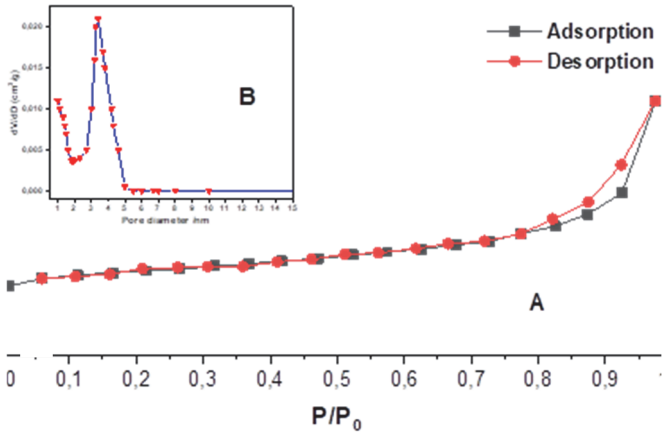

Fig. 6. N_2 adsorption–desorption isotherms (A) and BJH pore size distribution (B) diagrams of the Cs-$SiW_{11}Ru$ sample.

(CC) 2025 Serbian Chemical Society.

Isopropanol decomposition

The decomposition of isopropanol (IPA) without oxygen is frequently used as a chemical probe reaction to assess the acid–base characteristics of catalysts.[36,37] The decomposition of IPA leads to the formation of propene, diisopropyl ether (DIPE) or acetone. If the solid exhibits acidic properties, only the dehydration products (DIPE and propene) are obtained, whereas if the catalyst displays basic or redox properties, the dehydrogenation of the IPA occurs, resulting in the formation of acetone.[36,38]

Table II shows the results obtained from the IPA decomposition reaction using Cs-$SiW_{11}Ru$ as a catalyst as a function of reaction temperature. As shown in Table II, the conversion of isopropanol increases with the increasement of temperature. At all reaction temperatures, the catalyst exhibited high selectivity toward propene (only traces of acetone and diisopropylether were detected). This selectivity reached 99 % at a reaction temperature of 200 °C (Table II), indicating the presence of strong Lewis and/or Brønsted acid sites.[37,39] According to the literature,[40] the Lewis acidity of heteropoly salts result from metal ions, whereas the Brønsted acidity result from the presence of the residual unchanged protons and/or from water molecules coordinating metal cation that were introduced into heteropoly salts.

TABLE II. Results of the catalytic activity of Cs-$SiW_{11}Ru$ at different temperatures in IPA decomposition

t / °C	Conversion, %	Selectivity of products, %		
		Propene	Diisopropyl ether	Acetone
100	50	97	2	1
150	80	98	2	–
200	100	99	1	–

In other words, the solid Cs-$SiW_{11}Ru$ favoured dehydration over dihydrogenation; therefore, the solid Cs-$SiW_{11}Ru$ can essentially be assumed to be acidic.

Catalytic behavior

Effect of reaction temperature. The effect of the reaction temperature on CO_2 methanation was investigated in the range of 200–450 °C (in increments of 50 °C) at atmospheric pressure. The H_2/CO_2 ratio and the flow rate of the gas mixture were fixed at 4 and 1 L/h, respectively. The catalytic performance as a function of the reaction temperature is shown in Fig. 7, and the detailed catalytic results are summarized in Table S-I of the Supplementary material.

As shown in Fig. 7 and Table S-I, CO_2 conversion increases as the reaction temperature increases from 200 to 450 °C, reaching a maximum of 59 % at 450 °C. Fig. 7 also shows that at lower temperatures, *i.e.*, < 350 °C, the selectivities of methane and CO were 100 and 0 %, respectively. These results indicate that only the direct methanation mechanism occurs at low temperatures (from 200 to 300

(CC) 2025 Serbian Chemical Society.

°C). However, at the highest reaction temperatures (≥ 350 °C), there is a decrease in methane selectivity and an increase in CO selectivity, which can be attributed to the reverse water gas shift (RWGS) reaction ($CO_2 + H_2 \leftrightarrows CO + H_2O$, $\Delta H_{298\ K}$ = 41 kJ/mol), which becomes more favourable as the reaction temperature increases due to its endothermic nature. This result is in agreement with the results obtained in the literature.[41] Increasing the temperature is unfavourable since CO_2 methanation is highly exothermic, and it is important to operate at temperatures below 350 °C to achieve high methane selectivity at atmospheric pressure.

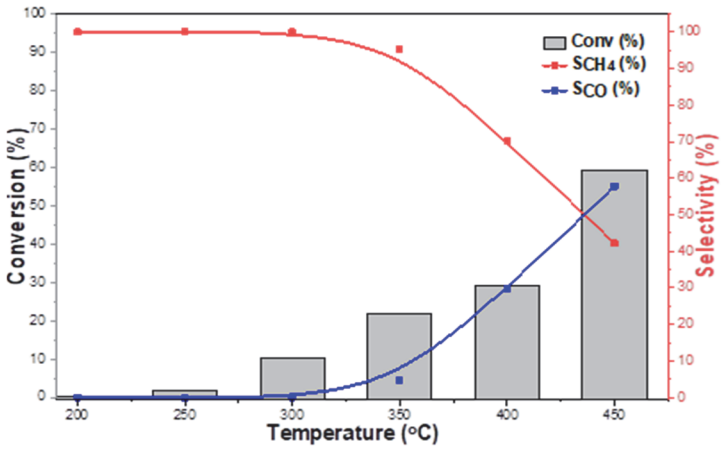

Fig. 7. Effect of temperature on CO_2 conversion and CH_4 selectivity. The reaction conditions were as follows: catalyst weight, 0.2 g; reaction temperature, 200–450 °C; H_2/CO_2, 4; flow rate, 1 L/h; and atmospheric pressure.

Effect of the flow rate of the reaction mixture. The effects of the reactant flow rate on CO_2 conversion and methane selectivity were studied in a reactor containing Cs-$SiW_{11}Ru$ at 300 °C with a stoichiometric reactant ratio (H_2/CO_2 = 4) by varying the flow rate of the reactant gases between 1 and 2 L/h. The results are shown in Fig. 8 and Table S-II of the Supplementary material.

As shown in Fig. 8, CO_2 the conversion and the CH_4 selectivity generally decreased as the reactant flow rate increased. Table S-II shows that when the flow rate was 1 L/h, the CO_2 conversion and methane selectivity obtained were 10 and 100 %, respectively. However, with a further increase in the flow rate to 2 L/h, the CH_4 selectivity and CO_2 conversion significantly decreased to 85.3 and 3 %, respectively. These observations could be explained by the shorter contact time between the reagents and the catalytically active sites, thus reducing the amount of reactants adsorbed onto the surface of the catalyst when the flow rate was increased. These results are in agreement with those of previous studies.[42,43]

(CC) 2025 Serbian Chemical Society.

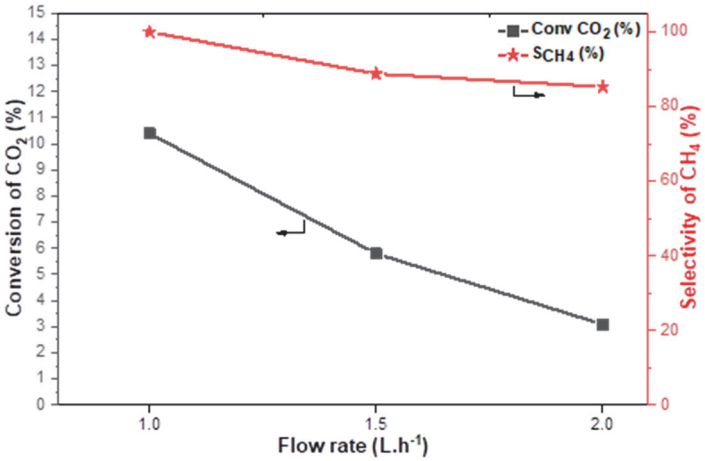

Fig. 8. Effect of the total flow rate on the performance of the Cs-SiW$_{11}$Ru catalyst. Reaction conditions: catalyst weight, 0.2 g; H_2/CO_2, 4; reaction temperature, 300 °C; atmospheric pressure.

Effect of the CO_2/H_2 ratio. To study the effect of the composition of the reaction mixture on the Cs-SiW$_{11}$Ru catalyst, several tests were carried out at 300 °C with a flow rate of 1 L/h, varying only the ratio of the reactive gases H_2/CO_2 from 1 to 4.

The results of the carbon dioxide conversion and methane selectivity as a function of the H_2/CO_2 ratio are shown in Fig. 9, and the detailed catalytic results are summarized in Table S-III of the Supplementary material. Fig. 9 shows that the conversion of CO_2 increases almost linearly with increasing H_2/CO_2 mole ratio from 1 to 4. For example, the conversion of CO_2 increases from 8 to 11 % when the H_2/CO_2 mole ratio is changed from 1 to 2 and reaches a maximum of 22.5 % when the H_2/CO_2 ratio is further increased from 2 to 4 (Table S-III). This result suggests that the increment of the H_2 content in the reactant mixture significantly enhances CO_2 conversion. Fig. 9 also shows the effect of the H_2/CO_2 mole ratio on CH_4 selectivity. The CH_4 selectivity slightly changed with increasing mole ratio. Table S-III shows that when the H_2/CO_2 mole ratio varies from 1 to 4, the CH_4 selectivity slightly increases from 98.1 % at a H_2/CO_2 ratio of 1 and reaches 100 % at a H_2/CO_2 ratio of 4. A further increase in the H_2 content slightly affects the CH_4 selectivity. These results show that the probability of CO_2 reacting with H_2 to form CH_4 is greater in the presence of a large amount of hydrogen. On the other hand, the formation of CO is favoured with a limited amount of hydrogen, as the methanation reaction remains incomplete. This observation could reinforce the results of earlier studies proposing a two-step reaction mechanism for the dissociation of CO_2 into CO_{ads} and O_{ads} before further reduction to CH_4.[44,45]

(CC) 2025 Serbian Chemical Society.

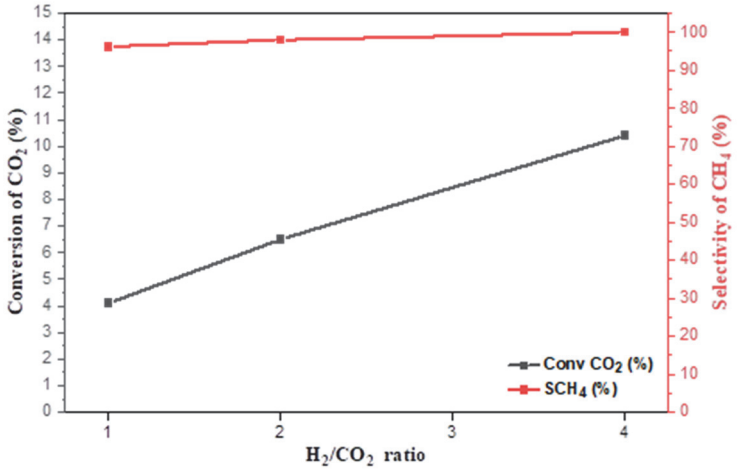

Fig. 9. Effect of the H_2/CO_2 ratio on the performance of the Cs-SiW_{11}Ru catalyst. The reaction conditions were as follows: catalyst weight, 0.2 g; flow rate, 1 L/h; reaction temperature, 300 °C; atmospheric pressure.

Effect of conversion on selectivity. Fig. 10 shows the evolution of methane and CO selectivities as a function of CO_2 conversion on the Cs-SiW_{11}Ru catalyst.

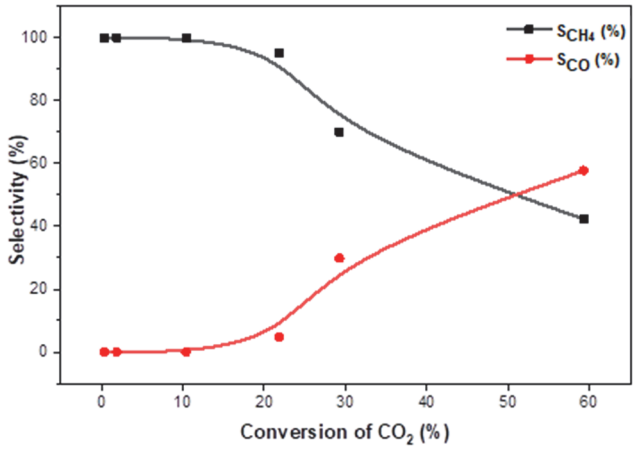

Fig. 10. Evolution of CH_4 and CO selectivities as a function of CO_2 conversion. Reaction conditions: catalyst weight, 0.2 g; temperature, 200–450°C; H_2/CO_2, 4; *P*, 1 atm; flow rate, 1 L/h.

Fig. 10 shows that when the conversion of CO_2 is less than 10 %, the selectivity for methane is 100 %, and that for CO is 0 %. However, the CO_2 conversion increased from 10 to 57.73 %, the selectivity of CH_4 drastically decreased to 42.27 %, and the CO selectivity increased from 0 to 57.73 %. This shows

(CC) 2025 Serbian Chemical Society.

that for the methanation of CO_2, CH_4 is the preliminary reaction product and is obtained by a series of consecutive reactions, whereas CO is the secondary reaction product.

Mechanism of CO_2 methanation

Although CO_2 methanation is a relatively simple reaction, its mechanism has not yet been clearly established. In general, two different mechanisms have been proposed for CO_2 methanation. The first mechanism involves the formation of CO as an intermediate product through the RWGS reaction, which is later converted into methane. The second mechanism involves the direct reaction of CO_2 with H_2 to form methane.[46,47] Several species, such as carbonates, hydrogen carbonates, formates and methoxys, have been identified on the surface of the catalyst. Various techniques, such as the temperature programmed desorption (TPD) and the Fourier transform infrared spectroscopy (FT-IR), have been used to identify all of these species.[48]

On the basis of effect of conversion on selectivity results (CH_4 was the preliminary reaction product) and the literature,[49] a mechanism involving the formation of surface is highly likely. Once the two reactants (CO_2 and H_2) are adsorbed on the surface of the catalyst, methane is obtained by the successive hydrogenation of several intermediates, including formate, dioxomethylene, and methoxy,[49] as shown in Scheme 1.

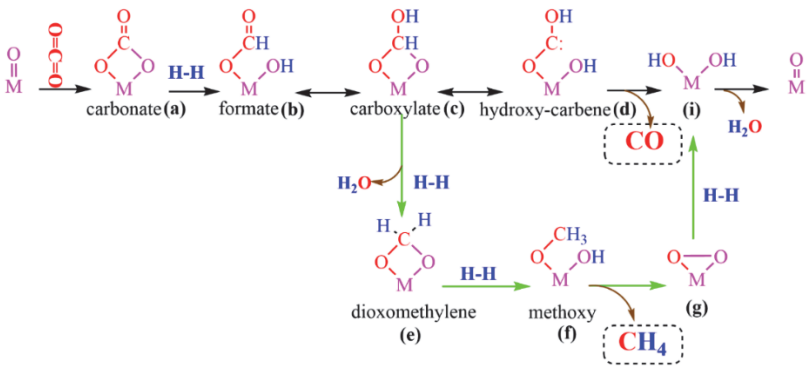

Scheme 1. Plausible mechanism of CO_2 methanation on Cs-SiW_{11}Ru.

After the surface is highly likely adsorption of CO_2 in the form of surface carbonate (a), the first step, which corresponds to the formation of formate species (b), is carried out relatively easily because it is energetically favourable. However, the successive hydrogenation of the formate to dioxomethylene (e) and then methoxy (f) groups is the rate-determining step (RDS) in methane synthesis. This step requires the most energy and is endothermic. The methoxy species (f) that leads to methane being strongly adsorbed on the surface of the catalyst, and the

(CC) 2025 Serbian Chemical Society.

temperature causes the methane to be desorbed by a radical process that leads to the formation of a peroxide species (g). Hydrogen addition enables the catalyst to be regenerated after a molecule of water has been eliminated.

Stability test

A catalytic test of 8 h at a reaction temperature of 300 °C was performed to assess the stability of the Cs-$SiW_{11}Ru$ catalyst as a function of time in the CO_2 methanation reaction. The results of the stability experiment are presented in Fig. S-3 of the Supplementary material. The Cs-$SiW_{11}Ru$ catalyst exhibited good stability, maintaining CO_2 conversion at approximately 10 % under operating conditions over the entire investigated time range. The CH_4 selectivity remained constant at 100 % throughout the stream. These results indicate that the catalyst was not subjected to deactivation during the tested period.

CONCLUSION

In the present study, a Cs-$SiW_{11}Ru$ catalyst was prepared by the reaction of the monolacunary silicotungstate (SiW_{11}) with $RuCl_3$ and CsCl. The product was characterized by FT-IR, UV and X-ray diffraction, indicating that it possesses Keggin structure. Finally, the catalyst was tested in a CO_2 methanation reaction at atmospheric pressure. The effects of several CO_2 methanation parameters, including the reaction temperature, H_2/CO_2 mole ratio and flow rate, on Cs-$SiW_{11}Ru$ were also investigated. With respect to the reaction temperature, an optimum range was found between 200 and 300 °C, because methane is the only molecule formed. In terms of the H_2/CO_2 molar ratio studied, our study revealed that CO_2 conversion increases continuously with the mole ratio, and the highest conversion is obtained for a stoichiometric ratio of 4. With respect to the flow rate, our study revealed that CH_4 selectivities remained unaffected while conversion decreased continuously with increasing flow rate, and the highest conversion was obtained for a flow rate of 1 L/h. In addition, this catalyst exhibited stable performance for 8 h of reaction. From this study, it can be concluded that the heteropolyanion system Cs-$SiW_{11}Ru$ is a promising catalyst for the conversion of CO_2 to methane, depending on the reaction conditions. The formate pathway proposed, where the CO_2 is converted to methane, involves: *i*) the adsorption of CO_2 in the form of surface carbonates which are rapidly hydrogenated to formiate intermediates, followed by *ii*) the successive hydrogenation of the formate to dioxomethylene then to methoxy species, and finally to methane.

SUPPLEMENTARY MATERIAL

Additional data and information are available electronically at the pages of journal website: https://www.shd-pub.org.rs/index.php/JSCS/article/view/13256, or from the corresponding author on request.

(CC) 2025 Serbian Chemical Society.

Acknowledgement. The authors would like to thank their colleagues (Pr. B. Bourahla and Dr. S. Sait from Tizi-Ouzou University - Algeria) for their support and useful discussions.

ИЗВОД

РУТЕНИЈУМ(III) МОНОСУПСТИТУИСАНИ ПОЛИОКСОВОЛФРАМАТ КЕГИНОВОГ ТИПА: СИНТЕЗА, КАРАКТЕРИЗАЦИЈА И ПРИМЕНА ЗА КАТАЛИТИЧКУ МЕТАНАЦИЈУ УГЉЕН-ДИОКСИДА

SADIA MANSOURI[1,2] и SALEM CHEKNOUN[1,3]

[1]Laboratory of Applied Chemistry, Faculty of Science, M. Mammeri University, BP 17 RP, 15000 Tizi-Ouzou, Algeria, [2]Department of Chemistry, Faculty of Sciences and Applied Sciences, A.M. Oulhadj University, 10000 Bouira, Algeria и [3]Department of Chemistry Faculty of Science, M. Mammeri University, BP 17 RP, 15000 Tizi-Ouzou, Algeria

$Cs_5[\alpha\text{-}SiW_{11}O_{39}Ru^{III}(H_2O)]\cdot 8H_2O$ со хетерополикиселине Кегинове структуре је успешно синтетисана, и њене физичкохемијске карактеристике су одређене дифракцијом X-зрака, UV–Vis спектроскопијом, инфрацрвеном спектроскопијом са Фуријеовом трансформацијом и Brunauer, Emmett и Teller анализом површине. Кисело–базне особине су одређене праћењем реакције разлагања изопропанола. Каталитичке перформансе за реакцију метанације CO_2 су испитане у реактору са фиксним слојем на атмосферском притиску уз варирање процесних параметара и то реакционе температуре (200–450 °C), молског односа реактаната H_2/CO_2 (1, 2 и 4) и брзине протока (1, 1,5 и 2 L/h). Експериментални резултати су показали да $Cs_5[\alpha\text{-}SiW_{11}O_{39}Ru^{III}(H_2O)]\cdot 8H_2O$ показује најбољи компромис између конверзије и селективности на 350 °C, при молском односу H_2/CO_2 од 4 и брзином протока 1 L/h.

(Примљено 18. фебруара, ревидирано 11. марта, прихваћено 7. маја 2025)

REFERENCES

1. T. Okuhara, N. Mizuno, M. Misono, *Adv. Catal*. **41** (1996) 113 (https://doi.org/10.1016/S0360-0564(08)60041-3)
2. R. Neumann, in *Progress in Inorganic Chemistry*, K. D. Karlin, Ed., John Wiley & Sons, Inc., New York, 1998 (https://doi.org/10.1002/9780470166482.ch3)
3. C.L Hill, *Chem. Rev.* **98** (1998) 1 (https://doi.org/10.1021/cr960395y)
4. I.V. Kozhevnikov, *Catalysts for fine chemical synthesis, catalysis by polyoxometalates*, Vol. 2, Wiley, Chichester, 2002
5. S. Hocine, C. Rabia, M. M. Bettahar, M. Fournier, *Stud. Surf. Sci. Catal.* **130** (2000) 1895 (https://doi.org/10.1016/S0167-2991(00)80478-4)
6. N. Dimitratos, J. C. Védrine, *Appl. Catal.* **81** (2003) 561 (https://doi.org/10.1016/S0920-5861(03)00154-8)
7. S. Cheknoun, S. Mansouri, O. Benlounes, S. Hocine, *J. Chem. Sci.* **130** (2018) 40 (https://doi.org/10.1007/s12039-018-1447-y)
8. S. Mansouri, O. Benlounes, C. Rabia, R. Touvenot, M. M. Bettahar, S. Hocine, *J. Mol. Catal., A* **379** (2013) 255 (https://doi.org/10.1016/j.molcata.2013.08.006)
9. G. Busca, F. Cavani, E. Etienne, E. Finocchio, A. Galli, G. Selleri, F. Trifirò, *J. Mol. Catal., A* **114** (1996) 343 (https://doi.org/10.1016/S1381-1169(96)00337-8)
10. H. S Jiang, X. Mao, S. J. Xie, B. K. Zhong, *J. Mol. Catal., A* **185** (2002) 143 (https://doi.org/10.1016/S1381-1169(01)00449-6)
11. P. Putaj, F. Lefebvre, *Coord. Chem. Rev.* **255** (2011) 1642 (https://doi.org/10.1016/j.ccr.2011.01.030)

(CC) 2025 Serbian Chemical Society.

12. S. Ogo, M. Miyamoto, Y. Ide, T Sano, M. Sadakane, *Dalton. Trans.* **41** (2012) 9901 (https://doi.org/10.1039/C2DT30475A)
13. A. Yokoyama, K. Ohkubo, T. Ishizuka, T. Kojima, S. Fukuzumi, *Dalton. Trans.* **41** (2012) 10006 (https://doi.org/10.1039/C2DT30424D)
14. A. M. Khenkin, I. Efremenko, L. Weiner, J. M. L. Martin, R. Neumann, *Chem. Eur. J.* **16** (2010) 1356 (https://doi.org/10.1002/chem.200901673)
15. L. Z. Zhang, Y. Q. Lu, M. Rostam-Abadi, *Phys. Chem. Chem. Phys.* **14 (**2012) 16633 (https://doi.org/10.1039/C2CP42209C)
16. B. S. Kwak, K. Vignesh, N. K. Park, H. J. Ryu, J. I. Baek, M. Kang, *Fuel* **143** (2015) 570 (https://doi.org/10.1016/j.fuel.2014.11.066)
17. P. H. Pandey, H. S. Pawar, *J. CO_2 Util.* **41** (2020) 101267 (https://doi.org/10.1016/j.jcou.2020.101267)
18. S. Li, L. Guo, T. Ishihara, *Catal. Today* **339** (2020) 352 (https://doi.org/10.1016/j.cattod.2019.01.015)
19. W. K Fan, M. Tahir, *J. Environ. Chem. Eng*. **9** (2021)105460 (https://doi.org/10.1016/j.jece.2021.105460)
20. W. Wei, G. Jinlong, *Front. Chem. Sci.* **5** (2011) 2 (https://doi.org/10.1007/s11705-010-0528-3)
21. A. Beuls, C. Swalus, M. Jacquemin, G. Heyen, A. Karelovic, P. Ruiz, *Appl. Catal., B* **113**–**114** (2012) 2 (https://doi.org/10.1016/j.apcatb.2011.02.033)
22. A. Karelovic, P. Ruiz, *Appl. Catal., B* **113**–**114** (2012) 237 (https://doi.org/10.1016/j.apcatb.2011.11.043)
23. Y. Li, Q. Zhang, R. Chai, G. Zhao, F. Cao, Y. Liu, Y. Lu, *Appl. Catal., A* **510** (2016) 216 (https://doi.org/10.1016/j.apcata.2015.11.034)
24. R. A. Hubble, J. Y. Lim, J. S Dennis, *Faraday Discuss.* **192** (2016) 529 (https://doi.org/10.1039/C6FD00043F)
25. S. Rönsch, J. Schneider, S. Matthischke, M. Schlüter, M. Götz, J. Lefebvre, P Prabhakaran, S. Bajohr, *Fuel* **166** (2016) 276 (https://doi.org/10.1016/j.fuel.2015.10.111)
26. A. Tézé, G. Hervé, *Inorg. Synth.* **27**(1990) 85 (https://doi.org/10.1002/9780470132586.ch16)
27. K. Filipek, *Inorg. Chim. Acta* **231** (1995) 237 (https://doi.org/10.1016/0020-1693(94)04347-X)
28. M. Sadakane, D. Tsukuma, M.H. Dickman, B. Bassem, U. Kortz, M. Higashijima, W. Ueda, *Dalton. Trans.* **35** (2006) 4271 (https://doi.org/10.1039/B606266K)
29. H. Chermette, F. Lefebvre, *C.R. Chimie* **15**(2012) 143 (https://doi.org/10.1016/j.crci.2011.09.002)
30. T. Okuhara, N. Mizuno, M. Misono, *Adv. Catal.* **41**(1996) 113 (https://doi.org/10.1016/S0360-0564(08)60041-3)
31. Y. Ding, Q. Gao, G. Li, H. Zhang, J. Wang, L. Yan, J. Suo, *J. Mol. Catal., A* **218** (2004) 161 (https://doi.org/10.1016/j.molcata.2004.04.019)
32. Q. Wu, X. Sang, F. Shao, W. Pang, *Mater. Chem. Phys.* **92** (2005) 16 (https://doi.org/10.1016/j.matchemphys.2004.07.026)
33. L. Méndez, R. Torviso, L. R. Pizzio, M. N. Blanco, *Catal. Today* **173** (2011) 32 (https://doi.org/10.1016/j.cattod.2011.03.028)
34. L. R. Pizzio, M. N. Blanco, *Micropor. Mesopor. Mat.* **103**(2007) 40 (https://doi.org/10.1016/j.micromeso.2007.01.036)
35. J. B. Moffat, *J. Mol. Catal*. **52**(1989) 169 (https://doi.org/10.1016/0304-5102(89)80088-4)

(CC) 2025 Serbian Chemical Society.

36. S. A. El-Molla, M. N. Hammed, G. A. El-Shobaky, *Mater. Lett*. **58** (2004) 1003 (https://doi.org/10.1016/j.matlet.2003.08.006)
37. H. G. El-Shobaky, A. S. Ahmed, N. R. E Radwan, *J. Colloids Surf., A* **274** (2006) 138 (https://doi.org/10.1016/j.colsurfa.2005.08.046)
38. C. Ancion, G. Poncelet, *Appl. Catal., A* **108** (1994) 31 (https://doi.org/10.1016/0926-860X(94)85178-6)
39. A. Gervasini, J. Fenyvesi, A. Auroux, *Catal. Lett.* **43**(1997) 219 (https://doi.org/10.1023/A:1018979731407)
40. M. Misono, *Catal. Rev. Sci. Eng*. **29** (1987) 269 (https://doi.org/10.1080/01614948708078072)
41. M. M. Jaffar, M. A. Nahil, P. T Williams, *Energy Technol.* **7** (2019) 1900795 (https://doi.org/10.1002/ente.201900795)
42. M. Gabrovska, R.Edreva-Kardijeva, D. Crisan, P. Tzvetkov, M. Shopska, I. Shtreva, *React. Kin. Mech. Catal.* **105** (2012) 79 (https://doi.org/10.1007/s11144-011-0378-0)
43. S. Abate, K. Barbera, Giglio E, F. Deorsola, S. Bensaid, S. Perathoner, R. Pirone, G. Centi, *Ind. Eng. Chem. Res.* **55** (2016) 8299 (https://doi.org/10.1021/acs.iecr.6b01581)
44. A. Borgschulte, N. Gallandat, B. Probst, R. Suter, E. Callini, D. Ferri, Y. Arroyo, R. Erni, H. Geerlings, A. Züttel, *Phys. Chem. Chem. Phys.* **15** (2013) 9620 (https://doi.org/10.1039/C3CP51408K)
45. S. Eckle, H. G. Anfang, R. J. Behm, *J. Phys. Chem., C* **115** (2011) 1361 (https://doi.org/10.1021/jp108106t)
46. E. Baraj, S. Vagaský, T. Hlinčík, K. Ciahotný, V. Tekáč, *Chem. Pap.* **70** (2016) 395 (https://doi.org/10.1515/chempap-2015-0216)
47. B. Miao, S. S. K. Ma, X .Wang, H. Su, S. H. Chan, *Catal. Sci. Technol.* **6** (2016) 4048 (https://doi.org/10.1039/C6CY00478D)
48. Z. M. Hu, K. Takahashi, H. Nakatsuji, *Surf. Sci.* **442** (1999) 90 (https://doi.org/10.1016/S0039-6028(99)00900-0)
49. H .Nakatsuji, Z. M. Hu, *Int. J. Quantum. Chem.* **77** (2000) 341 (https://doi.org/10.1002/(SICI)1097-461X(2000)77:1<341::AID-QUA33>3.0.CO;2-T).

(CC) 2025 Serbian Chemical Society.